

Published in final edited form as:

*J Pharm Sci.* 2015 February ; 104(2): 416–423. doi:10.1002/jps.24132.

## Stability Analysis of an Inline Peptide-based Conjugate for Metal Delivery: Nickel(II)-*cla*MP Tag Epidermal Growth Factor as a Model System

Brittney J. Mills<sup>1</sup> and Jennifer S. Laurence<sup>2,\*</sup>

<sup>1</sup>Department of Chemistry, The University of Kansas, Lawrence, KS 66045

<sup>2</sup>Department of Pharmaceutical Chemistry, The University of Kansas, Lawrence, KS 66047

### Abstract

Metals are a key component of many diagnostic imaging and biotechnology applications, and the majority of cancer patients receive a platinum-based drug as part of their treatment. Significant effort has been devoted to developing tight binding synthetic chelators to enable effective targeted delivery of metal-based conjugates, with most successes involving lanthanides rather than transition metals for diagnostic imaging. Chemical conjugation modifies the protein's properties and generates a heterogeneous mixture of products. Chelator attachment is typically done by converting the amino group on lysines to an amide, which can impact the stability and solubility of the targeting protein and these properties vary among the set of individual conjugate species. Site-specific attachment is sought to reduce complexity and control stability. Here, the metal abstraction peptide (MAP) technology was applied to create the *cla*MP Tag, an inline platform for generating site-specific conjugates involving transition metals. The *cla*MP Tag was genetically encoded into epidermal growth factor (EGF) and loaded with nickel(II) as a model system to demonstrate that the tag within the homogeneous inline conjugate presents sufficient solution stability to enable biotechnology applications. The structure and disulfide network of the protein and chemical stability of the *cla*MP Tag and EGF components were characterized.

### Keywords

PROTEIN STRUCTURE; STABILITY; CONJUGATION; TARGETED DRUG DELIVERY; METAL ABSTRACTION PEPTIDE; MAP; ABSORPTION SPECTROSCOPY; NMR; CHROMATOGRAPHY; ANALYTICAL BIOCHEMISTRY

\*To whom correspondence should be addressed: Dr. Jennifer S. Laurence, Multidisciplinary Research Building, The University of Kansas, 2030 Becker Drive, Lawrence, KS 66047, Tel: 785-864-3405, Fax: 785-864-5736, laurencj@ku.edu.

#### SUPPORTING INFORMATION

This article contains supplementary material available from the authors upon request or via the Internet at <http://onlinelibrary.wiley.com/>.

#### CONFLICT OF INTEREST STATEMENT

JSL is co-owner of Echogen Inc., a limited liability company that has licensed the patent-protected metal abstraction peptide (MAP) technology from the University of Kansas.

## INTRODUCTION

Coupling of chelators to proteins allows for the generation of conjugates that enable metal-based imaging or therapeutic applications.<sup>1-3</sup> Generally this requires optimization of linker chemistry and additional purification steps to obtain the desired product.<sup>1,4-6</sup> Even though the conjugated entities are much smaller in size than the protein molecule, the impact of their addition may not be insignificant. These alterations often affect pharmaceutical properties, including solubility, chemical and physical stability, and colloidal behavior of the protein.<sup>7</sup> The magnitude and type of effect depends on the specific position modified and the structural attributes of the protein,<sup>8</sup> as well as the properties of the linker and attached compound.

The physical stability of proteins depends on the core structure, packing interactions and surface composition. The surface properties that develop in the folded state affect solubility and colloidal stability, but they also determine solvent access to core structural elements that contribute to the overall three-dimensional fold and aggregation propensity of the molecule.<sup>9</sup> As such, the composition of the molecule's surface significantly impacts its stability, which is altered by conjugation. This principle is apparent when comparing homologous proteins or mutants having the same three-dimensional fold because each variant can exhibit widely different stability profiles depending on their distinct surface properties.<sup>10,11</sup> Charged residues located on the surface of structured proteins often increase the physical stability by protecting against thermal unfolding<sup>10,11</sup> or by decreasing aggregation propensity due to charge-charge repulsion between protein molecules.<sup>12</sup> Conjugation to surface-exposed lysine residues is commonly used in formation of bioconjugates, and it alters the surface charge and causes large product heterogeneity.<sup>13</sup> Even though conjugates are successfully formed using this chemical method, altering the surface charge can affect the stability of the molecule<sup>7,14</sup> and also introduce unexpected complexity, as multiple charge states have been observed when modifying a single lysine, depending upon its position in the structure.<sup>15</sup> To be able to control and/or better characterize stability, conjugation to native or engineered cysteine residues and non-natural amino acids has been pursued to increase site specificity.<sup>16</sup> Modification of native cysteine residues in antibodies has been performed by reducing inter-strand disulfide bonds and conjugating at these positions. Heterogeneity is decreased greatly compared to lysine-based approaches, but complexity remains and physical stability can be adversely affected.<sup>8,17,18</sup> Introduction of additional cysteine residues permits site-specific attachment, and the THIOMAB approach has demonstrated success in identifying suitable positions within antibodies for this purpose.<sup>19</sup> Site-specific attachment of any type permits detailed analysis of the structure and stability of the protein conjugate, allowing for selection of desirable attributes.

The *cla*MP Tag is based on the metal abstraction peptide (MAP) composed of the amino acid sequence Asn-Cys-Cys (NCC).<sup>20-22</sup> It has been shown to bind Ni(II), forming a single specific metal-peptide complex structure having an overall charge of 2<sup>-</sup><sup>20</sup> and unusual binding and release properties.<sup>23</sup> Incorporation of the NCC module into longer peptide sequences has been shown to have no discernable effect on complex formation.<sup>22</sup> Therefore, the *cla*MP Tag can be biosynthetically encoded into a protein to generate a linker-less bioconjugate,<sup>24</sup> which eliminates the need to chemically link to a chelating moiety. The

specific metal abstraction chemistry performed by NCC occurs with a variety of transition metal ions.<sup>23</sup> The *claMP* Tag also binds cytotoxic metals, such as Pt and Pd, and radioisotopes, such as <sup>99m</sup>Tc, <sup>64/67</sup>Cu, and <sup>60</sup>Co (unpublished data); thus, it has the potential to serve as a metal-binding agent for use in a variety of imaging and therapeutic applications.

Our previous study demonstrated that the *claMP* Tag can be successfully incorporated at different positions within a thiol- and disulfide-containing fusion protein composed of thioredoxin and epidermal growth factor (EGF) without any negative effects on the expression yield, structure, or function of the tagged protein.<sup>24</sup> Herein is presented the solution stability of this model system, the Ni(II)-*claMP*-EGF conjugate and the Ni-*claMP* Tag module in the context of the EGF system, to demonstrate the potential of the *claMP* Tag in serving as an inline metal carrier. The inline Ni-conjugates were stored in aqueous solution using two different buffers, and UV-vis absorption spectroscopy, liquid chromatography, mass spectrometry, NMR, circular dichroism, and static light scattering were used to characterize stability and changes in the conjugate structure over a 24-week period.

## EXPERIMENTAL METHODS

### Protein Expression and Purification

Wild-type and *claMP* Tag constructs were expressed and purified as previously described.<sup>24</sup> Briefly, the DNA sequence was inserted into the pET-32Xa vector using a pET-32Xa/LIC cloning kit (Novagen). The plasmid was transformed into the Origami B (DE3) cell strain (Novagen) followed by expression in either *Luria Broth* or MMTM (for NMR samples). All of the samples for NMR analysis were grown on <sup>15</sup>N-labeled ammonium chloride (Isotech) as the nitrogen source. After expression, a 1 L pellet was resuspended, lysed using a French Press, and purified using a Hi-Trap Chelating HP column (GE Healthcare) charged with Ni(II). Cleavage with thrombin and Factor Xa (Novagen) were completed to obtain the final product. Protein concentration was determined using the Bradford assay, and the samples were concentrated to approximately 0.2 mM. EGF and EGF-Ni-*claMP* were each prepared in either 50 mM Tris-Cl, 10 mM NaCl, pH 7.3 or 50 mM potassium phosphate (KPi), 10 mM NaCl, pH 7.3 and stored at 4 °C.

### Absorption Analysis

UV-vis spectroscopy was used to monitor Ni(II) incorporation into the *claMP* Tag and were interpreted as described previously.<sup>20</sup> Samples were placed in a 1-cm path length cuvette. Spectra were acquired from 200-800 nm using a Cary 100 Bio UV-visible spectrophotometer (Varian). Quantitation of the absorbance at 310 nm was used to determine the amount of intact Ni(II)-*claMP* Tag in solution.

### Size Exclusion Chromatography (SEC)

Size exclusion chromatography was used to assess the purity of the sample and determine if larger molecular weight species formed over time. Analysis was performed using a 4.6×300 mm Yarra SEC-2000, 3 μm pore size column (Phenomenex). The column was equilibrated

in “Buffer A” (20 mM Tris-Cl, 10 mM KCl, pH 7.5 before injection of the sample. A constant flow rate of 0.35 mL/min “Buffer A” over 40 minutes was used to elute the protein from the column. UV absorption at 220 nm was used to monitor protein elution from the column. The area of the peak at 8 minutes was used to quantify the amount of monomer at each incubation time point.

### Anion Exchange Chromatography (AEC)

AEC was performed using a 4.6×250 mM BioLC ProPac WAX-10 column (Dionex). Before sample injection, the column was equilibrated using “Buffer A”. Protein was eluted using a linear gradient from 0-100% “Buffer B” (“Buffer A” + 500 mM KCl) over 70 minutes. A constant flow rate of 1 mL/min was used, and UV absorption at 220 nm was used to monitor protein elution from the column. The area of the main peak at 75 minutes was used to estimate the amount of protein present. Fluctuations in peak area of approximately 20% were observed for duplicate samples analyzed on the same day. Because large run-to-run instrument variation in absorbance was observed, the elution profile was used to establish trends and not for absolute quantitation.

### <sup>1</sup>H-<sup>15</sup>N HSQC NMR

To examine the structural stability of the constructs using 2D NMR, EGF and EGF-Ni-*cl*aMP were prepared in two buffer systems at pH 7.3, 50 mM Tris-Cl or 50 mM KPi, each containing 10 mM NaCl and 6% D<sub>2</sub>O. The samples were concentrated to approximately 0.1 mM for analysis. <sup>1</sup>H-<sup>15</sup>N Heteronuclear Single Quantum Coherence (HSQC) spectra were acquired on a 600 MHz Bruker Avance NMR spectrometer with a triple resonance cryoprobe. The spectra for EGF-Ni-*cl*aMP were acquired with 120 and 217 scans for the samples prepared in Tris-Cl and KPi, respectively, with 2048 points in <sup>1</sup>H and 128\* increments in <sup>15</sup>N. The numbers of scans used were selected to account for variations in sample concentration and achieve a similar signal to noise ratio of approximately 100:1. All spectra were obtained at 25 °C. Spectra were obtained at multiple time intervals to evaluate time-dependent changes to protein structure. NMRpipe<sup>25</sup> and SPARKY<sup>26</sup> were used to process the spectra and for data analysis. Comparison of line widths at half height was performed to establish the proteins were monomeric and relative peak heights were assessed to determine the amount of protein remaining in the sample as a function of time.

### Static Light Scattering and Intrinsic Fluorescence

Static light scattering (SLS) and intrinsic fluorescence were collected using a Photon Technology International (PTI) QM-40 spectrofluorometer (Birmingham, NJ) equipped with a four-position sample holder and a Peltier temperature controller (Quantum Northwest). Samples were prepared at a protein concentration of 0.5 mg/mL in 50 mM KPi, 10 mM NaCl, pH 7.3 and loaded in 0.2 cm × 1 cm path length quartz cuvettes (Starna Cells). The intensity of scattered light at the excitation wavelength of 295 nm was detected by a photomultiplier tube at an angle 90° to the light source. Intrinsic fluorescence data was acquired simultaneously during the static light scattering experiments using a second photomultiplier located 180° to the static light scattering detector and monitoring the emission from 310 nm to 390 nm. Emission spectra were collected every 2.5 °C from a

temperature range of 5 to 80 °C, with a two-minute equilibration at each temperature. Data was collected every 1 nm using a 1 second integration time at each wavelength. Fluorescence and scattering from the buffer alone were subtracted from all measurements. Two samples were analyzed for each variant.

### Circular Dichroism

Circular dichroism (CD) measurements were performed using a Chirascan spectropolarimeter (Applied Photophysics, Surrey, UK) equipped with a four-position sample holder and a Peltier temperature controller (Quantum Northwest). Samples were prepared at a protein concentration of 0.035 mg/mL in 50 mM KPi, 10 mM NaCl, pH 7.3 and loaded into a 0.1-cm path length quartz cuvette (Starna Cells). Spectra were acquired every 2.5 °C from 5 to 80 °C, with a one-minute equilibration at each temperature. An averaging time of 0.5 seconds/nm and a bandwidth of 1 nm were used. The molar ellipticity at 200 nm was plotted as a function of temperature. CD signals from the buffer alone were subtracted from all measurements. Two samples were analyzed for each variant.

## RESULTS AND DISCUSSION

Here, *cla*MP-Tagged EGF was used as a model system to analyze the stability of the *cla*MP Tag in the context of a protein system and verify that incorporation of the *cla*MP Tag does not substantially adversely affect protein stability. The tag rapidly becomes fully occupied in the presence of the metal transfer agent, efficiently yielding a highly stable single species in solution.<sup>20,22,24</sup> Nonetheless, in the event of incomplete loading the metal-occupied *cla*MP-Tagged protein may be separated easily from any residual unreacted proteins using ion exchange chromatography because the correctly formed Ni(II) complex develops a 2<sup>-</sup> charge, differentiating it from the unoccupied form. This approach efficiently generates a single, homogeneous conjugate species, permitting the stability of the resulting product to be well characterized.

### Stability of EGF and Ni-*cla*MP Tag within the Conjugate

The stability of the metal-bound *cla*MP Tag is important to investigate in order to successfully implement the tag as an inline conjugate for therapeutic and diagnostic purposes. Biologics and conjugates must be stable in solution for 1-2 months to retain activity during manufacture and administration and for up to two years if formulated as a liquid. Most biologics, however, are stored as frozen and/or dried formulations to best preserve their integrity during the required shelf life. Accelerated stability studies of ADCs have demonstrated that linking drugs molecules to antibodies leads to formation of high molecular weight species (HMWS) and diminished structural stability.<sup>8,17</sup> In this system dimers or HMWS have the potential to result from either covalent crosslinking via disulfide bond formation or Ni-based oxidation or bridging via the metal upon liberation from the tag. SEC was used to investigate formation of multimers over time. In the initial chromatogram, EGF-Ni-*cla*MP elutes as a fully monomeric species exhibited by one main peak at 7.5 minutes (Figure 1). This is in contrast to native EGF under the same low salt condition, which displays an unusual profile consisting of two peaks eluting at approximately 8.5 and 9.5 minutes. The presence of the two peaks is dependent on buffer concentration, such that

analysis of EGF on the SEC column at slightly higher buffer concentration (30 mM Tris, 15 mM KCl) yields a broad single peak at 9.0 min (data not shown). The expected explanation would be that dimerization of native EGF is favored at low ionic strength and that addition of the tag inhibits dimer formation. Analysis of the line widths of the NMR data for both proteins, however, indicates only monomer is present in each sample (data not shown). Because increased ionic strength eliminates the double peak and the protein recovered from the column is uniformly monomeric, these peaks likely represent two exchangeable conformers. The presence of only one peak in the *cla*MP-Tagged EGF chromatogram suggests the protein's structural flexibility may be restricted to a single conformation in the presence of the negatively charged tag, which is adjacent to a patch of basic residues.<sup>24</sup> At the 12-week time point, the EGF-Ni-*cla*MP peak shape is slightly altered, gaining a shoulder peak centered at 8.4 minutes, corresponding to a smaller molecular weight species or the emergence of a second conformer, as observed with EGF. These SEC data show no evidence of dimers or HMWS even at 24 weeks. Earlier eluting species indicative of protein crosslinking or aggregation are not present, implying the global conformation and the Cys residues within EGF-Ni-*cla*MP are unaltered. The presence of Ni(II) has been observed to cause oxidative crosslinking of proteins.<sup>27</sup> As such, the SEC data further implies that nickel is not released readily from the *cla*MP Tag because dimers and HMWS do not emerge.

To investigate changes in the Ni-*cla*MP complex, such as loss of metal or alteration of the ligands around the metal center, absorption spectroscopy and charge-based separation was used. The nickel(II) complex was used to perform this initial stability study because its absorption spectrum is rich in structural detail,<sup>22</sup> and any chemical or structural transformation of the Ni-*cla*MP complex would alter the features in the UV-vis spectrum and the unique 2<sup>-</sup> charge of the complex. The UV-vis absorption data shows that EGF-Ni-*cla*MP is stable over a 12-week period, as no decreases in peak height were observed for the protein and Ni-*cla*MP features (Figure 2). After 24 weeks, a decrease in intensity of the feature at 310 nm, which corresponds to the ligand-metal charge transfer band from the Ni-*cla*MP complex, is observed. Because correct formation of the *cla*MP complex introduces a change in charge of 2<sup>-</sup>, Ni-*cla*MP-Tagged EGF exhibits a significantly different elution profile than EGF when separated on an anion exchange column. AEC was used to cross-validate the stability of Ni-*cla*MP by evaluating the elution profile of soluble *cla*MP-Tagged EGF over time. EGF elutes at approximately 35 minutes, whereas EGF-Ni-*cla*MP elutes at 75 minutes. Samples prepared in either 50 mM Tris-Cl, pH 7.3 or 50 mM KPi, pH 7.3, each containing 10 mM NaCl, exhibited the same chromatographic feature at the initial time point, confirming the conjugate has the same surface charge regardless of the buffer system in which it is prepared (Figure 3). This supports the SEC data, confirming the buffer choice does not noticeably impact the behavior of the molecule.

Like native EGF, the AEC peak area of EGF-Ni-*cla*MP prepared in either buffer is constant through eight weeks within instrument variability (+/- 20%), indicating the protein remains intact and soluble. Peak area for these preparations decreased below the variability threshold to approximately 25% and 35% at the 12-week time point for samples prepared in Tris-Cl and KPi, respectively (Figure 3). Multiple replicates were analyzed, and peak areas acquired from the same sample and different batches were observed to deviate substantially at the

same time point. A 15-35% decrease in peak area was observed at the 12-week time point depending on the sample analyzed. Because the AEC peak area values were extremely variable, this data was not useful for absolute quantitation and instead was used solely in a qualitative manner to identify general trends and changes in the profile. EGF-Ni-*cla*MP prepared in KPi exhibits a downward trend in peak area starting at the 12-week time point, while the sample prepared in Tris-Cl also decreases in peak area, although to a lesser extent. The AEC analysis shows that Ni(II) is retained by the *cla*MP complex but also indicates that after longer periods of time a change in charge occurs. There is the emergence of an additional peak around 50 minutes in the AEC chromatogram of the sample prepared in KPi at the 12-week time point, and this feature grows in intensity at later time points. Because earlier elution indicates a specie is less negatively charged than the conjugate, this data suggests a cleavage event, likely resulting in removal of the Ni-*cla*MP complex, and/or alterations in the protein structure near this region has occurred.

### Identification of Cleavage Fragment

To further investigate the possible cleavage event and determine if it leads to removal of the Ni-*cla*MP complex from EGF, mass spectrometry (MS) was performed. MS analysis of the sample after 24 weeks reveals hydrolysis of the peptide backbone occurs following L52 and preceding R53, the C-terminal residue of the native EGF sequence. This validates the SEC data, which shows emergence of a smaller molecular weight species. It also aligns with the AEC results, which indicate the degradant is less negatively charged than the conjugate but more negative than native EGF. EGF without its terminal Arg and the Ni-*cla*MP complex would exhibit a charge of 5<sup>-</sup>, causing it to elute later than native EGF but earlier than EGF-Ni-*cla*MP. The MS data support hydrolytic cleavage of the peptide backbone. Because of the large variability observed between different sample preparations in the rate at which this species emerges and that cleavage occurs between Leu52 and Arg53, we hypothesize the primary degradant observed is caused by a minor, undetectable protease contaminant. Because in our previous short-term studies no evidence of proteolysis had been observed, the same purification approach was used. To better protect against proteolytic contamination, additional purification steps and protease inhibitors could be added to optimize the purification, as would be done when generating a therapeutic product. Both chymotrypsin and pepsin have been shown to cleave on the C-terminal side of leucine,<sup>28</sup> which is consistent with the location of cleavage in this EGF conjugate. Evidence of metal-induced hydrolysis has been reported to occur in the presence of various ions, including Ni(II).<sup>29</sup> This is specific to the sequence SHHK and depends on the presence of one of two embedded His. Complete cleavage occurs in a substantially shorter time frame, suggesting that it is not the same mechanism. Because the Ni(II)-*cla*MP Tag system undergoes a long lag period before degradation begins, it is likely that the eventual release of a small amount of Ni(II) activates a proteolytic contaminant. Even in this sub-optimized liquid sample, cleavage is minimal up to two months. For research applications, this provides sufficient time to carry out most analyses, and for example, if <sup>57</sup>Ni is inserted for use in medical imaging,<sup>30,31</sup> the radioisotope would be inserted into the tag in the nuclear pharmacy, and the image would be acquired long before cleavage would occur in the formulation. In addition, it is clear that despite the presence of molecular oxygen in the samples throughout the incubation, no evidence of oxidation (e.g. methionine sulfoxide) was detected in the MS

data, indicating the presence of the Ni-*cla*MP Tag complex does not lead to chemical incorporation of oxygen into the targeting protein even after 24 weeks.

The emergence of the cleaved fragment is accompanied by a small amount of visible precipitation. The absorption at 280 nm remains constant at 24 weeks, but the absorption of the Ni-*cla*MP feature at 310 nm decreases, suggesting selective precipitation of the Arg53-Ni-*cla*MP fragment. Analysis of the NMR peak intensities also confirms precipitation of neither EGF nor EGF-Ni-*cla*MP occurs. It was determined previously that the cysteine residues are unaltered by addition of the tag, and as such, these resonances can be used to quantify the total amount of soluble monomeric protein in the sample. The peak heights of the cysteine residues in the HSQC spectra remain constant over the 24-week period, confirming the intact EGF-Ni-*cla*MP and cleaved EGF components remain in solution. The peak heights corresponding to Arg53 and the added Gly from the *cla*MP Tag decrease in intensity over the 24-week time period, further indicating precipitation of the cleaved Arg53-Ni-*cla*MP Tag fragment occurs (Figure 4). Because the net charge of the Arg53-Ni-*cla*MP fragment is 1<sup>-</sup>, presuming no other alterations, its aqueous solubility may be limited, particularly in the presence of the highly soluble, negatively charged protein, as might be predicted based on general principles and other peptides.<sup>11</sup>

The likelihood of this cleavage event occurring with a *cla*MP-Tagged bioconjugate can be reduced by various standard measures, including frozen storage, lyophilization, and improving purification procedures to better eliminate proteolytic contaminants derived from the host, in this case *E. coli*. In this study, a simple two-step purification was used, and no additional precautions were taken to inhibit proteases, chelate residual or released metal, or eliminate oxygen and light exposure during storage. Follow-up studies to examine each parameter individually are being pursued to characterize in greater detail their influence on conjugate stability. In the construct examined here, a glycine spacer was included between EGF and the tag. Examination of a matrix of synthetic peptides and tagged protein variants has shown the spacer is unnecessary for metal complex formation (unpublished data), indicating the spacer may be removed or substituted. As such, if a spacer is desired, residues less prone to rapid cleavage than Gly can be utilized to reduce potential proteolysis. Based on this initial study, which demonstrates very good stability of the complex, optimization of these external factors will allow for the formation of highly stable *cla*MP-Tagged bioconjugates. The basal conditions analyzed provide a good starting point for identifying stable formulation conditions, which is an important consideration in the development of bioconjugates utilizing the *cla*MP Tag technology.

### Impact of the *cla*MP Tag on the Structural Stability of EGF

Because SEC showed the EGF proteins remained entirely monomeric and soluble at 24 weeks, 2D heteronuclear NMR was used to more closely investigate the local structural stability of *cla*MP-Tagged EGF. The <sup>15</sup>N-<sup>1</sup>H HSQC NMR experiment is the most accurate tool that can be applied to analyze protein structure in solution because it is a highly sensitive reporter of the entire backbone conformation.<sup>32-34</sup> It has previously been shown that addition of the thiol-containing sequence to the C-terminus of EGF does not negatively impact native disulfide bond formation or the higher order structure of the molecule.<sup>24</sup> Here,



the initial  $^1\text{H}$ - $^{15}\text{N}$  HSQC spectra of EGF-Ni-*cla*MP prepared in each buffer are nearly identical, confirming the tertiary structure of EGF-Ni-*cla*MP is not altered by buffer selection (Figure 5), consistent with SEC and AEC results. At the 12-week time point, additional peaks emerge near the initial resonance positions corresponding to the backbone amides from C-terminal residues W49, W50, E51, and L52. The indole NH from the side chains of W49 and W50 begin to split from one overlapped peak into two. One of these sets of peaks must correspond to the two Trp within the cleaved EGF product. Because of the intensity of these NMR peaks and because the MS data shows only two masses, the other NMR peaks must represent a slightly altered conformational state. This second set of peaks may reflect the cleaved product rather than the full-length species because a peak corresponding to the position of L52 in EGF appears and an additional peak in close proximity to it also emerges, suggesting a very small conformational adjustment. These limited site-specific changes become more distinct at the 24-week time point, yet the global structure and disulfide network of the protein remain the same (Figure 6). Based on the NMR data, it is clear that there are no significant tertiary structure alterations to the protein over time, with the exception of the C-terminal cleavage event confirmed by MS.

Altering the surface properties of the molecule through *cla*MP Tag addition did not significantly affect the structure or stability of EGF. Although EGF is a model system and it has little regular structure, thermal titration of EGF and EGF-Ni-*cla*MP were performed to verify that adding the tag did not alter appreciably the unfolding and aggregation behavior of the parent protein. The unusual fold of EGF produces a CD spectrum with atypical features. The CD features of Ni-*cla*MP overlap extensively with EGF above 220 nm and are opposite in sign, leading to the absence of an informative signal in this portion of the spectrum (Supp. Fig. 1a). As such, unfolding of EGF was monitored at 200 nm to detect changes in random coil. With and without the tag, EGF behaved identically (Supp. Fig. 1b). The onset temperature for unfolding ( $T_{m,\text{onset}}$ ) is indicative of the physical instability of the conjugate, as reported for ADCs.<sup>8</sup> As such, the fact that the  $T_{m,\text{onset}}$  values of *cla*MP-Tagged EGF and native EGF are indistinguishable, indicates that incorporation of the *cla*MP Tag is innocuous. Intrinsic Trp fluorescence also was monitored as a function of temperature (data not shown). EGF has two Trp residues, both located near the C-terminus. Despite the obvious chemical shift change to these residues detected by NMR, no difference in fluorescence was observed between the two proteins, suggesting only a minor adjustment to the conformation or dynamic properties occurs. Visible precipitation was not observed and unfolding was reversible for both species. SLS was used to monitor formation of aggregates as a function of temperature, but no scattering could be detected for either protein up to the maximum temperature of 80 °C. Because native EGF is highly negatively charged, it is not unexpected that making it more negative by addition of the Ni-*cla*MP complex does not diminish stability. Charge repulsion and retention of the disulfide bonds likely protects EGF from both non-native and colloidal aggregation. In the context of this system, alterations in surface charge due to *cla*MP Tag addition were shown to have minimal effects on protein stability, which is promising for application of this tag in biotechnology applications. Of course, each system to which the *cla*MP Tag is applied would need to be investigated to characterize the impact on that specific molecule. Additional studies are ongoing to evaluate

the effects on stability of incorporating the *cla*MP Tag into a diverse set of proteins that vary in isoelectric point, size, charge, and architecture.

## CONCLUSION

In this study, the Ni(II)-*cla*MP Tag complex was shown to retain metal binding and not negatively alter the higher order structural stability of the protein molecule to which it is attached. Although cleavage of the Arg53-Ni-*cla*MP fragment occurs, there is a two-month lag before onset, suggesting degradation can be mitigated by increasing sample and/or reagent purity as well as storing it frozen and/or dried. Therefore, this stability analysis of the EGF-Ni-*cla*MP conjugate confirms that the *cla*MP Tag module is structurally and chemically stable and does not adversely impact the physicochemical stability of the protein to which it is attached, here EGF.

## Supplementary Material

Refer to Web version on PubMed Central for supplementary material.

## ACKNOWLEDGEMENTS

Funding was provided by Wallace H. Coulter Foundation (CTRA) and KU Cancer Center Pilot Award. NIGMS Biotechnology Predoctoral Training Grant (T32 GM-08359) provided support for B.J.M. The authors thank Drs. C.R. Middaugh, D. Volkin, and O. Kumru for use of equipment and assistance with CD, SLS, and fluorescence data collection and the KU Mass Spectrometry lab for analyzing the mass spectrometry samples.

## REFERENCES

1. De León-Rodríguez LM, Kovacs Z. The Synthesis and Chelation Chemistry of DOTA-Peptide Conjugates. *Bioconjugate Chem.* 2008; 19(2):391–402.
2. Breeman WAP, Kwekkeboom DJ, de Blois E, de Jong M, Visser TJ, Krenning EP. Radiolabelled regulatory peptides for imaging and therapy. *Anti-Cancer Agents Med Chem.* 2007; 7(3):345–357.
3. Wängler C, Buchmann I, Eisenhut M, Haberkorn U, Mier W. Radiolabeled peptides and proteins in cancer therapy. *Protein Pept Lett.* 2007; 14(3):273–279. [PubMed: 17346233]
4. Knör S, Modlinger A, Poethko T, Schottelius M, Wester H-J, Kessler H. Synthesis of novel 1,4,7,10-tetraazacyclodecane-1,4,7,10-tetraacetic acid (DOTA) derivatives for chemoselective attachment to unprotected polyfunctionalized compounds. *Chem - Eur J.* 2007; 13(21):6082–6090. S6082/6081-S6082/6020. [PubMed: 17503419]
5. Lewis MR, Kao JY, Anderson A-LJ, Shively JE, Raubitschek A. An improved method for conjugating monoclonal antibodies with N-Hydroxysulfosuccinimidyl DOTA. *Bioconjugate Chem.* 2001; 12(2):320–324.
6. Lewis MR, Raubitschek A, Shively JE. A Facile, Water-Soluble Method for Modification of Proteins with DOTA. Use of Elevated Temperature and Optimized pH To Achieve High Specific Activity and High Chelate Stability in Radiolabeled Immunoconjugates. *Bioconjugate Chem.* 1994; 5(6):565–576.
7. Wakankar AA, Feeney MB, Rivera J, Chen Y, Kim M, Sharma VK, Wang YJ. Physicochemical Stability of the Antibody-Drug Conjugate Trastuzumab-DM1: Changes due to Modification and Conjugation Processes. *Bioconjugate Chem.* 2010; 21(9):1588–1595.
8. Beckley NS, Lazzareschi KP, Chih H-W, Sharma VK, Flores HL. Investigation into Temperature-Induced Aggregation of an Antibody Drug Conjugate. *Bioconjugate Chem.* 2013; 24(10):1674–1683.

9. Laurence, JS.; Middaugh, CR. Fundamental structures and behaviors of proteins. In: Wang, W.; Roberts, CJ., editors. *Aggregation of Therapeutic Proteins*. Hoboken, NJ: John Wiley & Sons, Inc; 2010. p. 1-61.
10. Dominy BN, Minoux H, Brooks CL III. An electrostatic basis for the stability of thermophilic proteins. *Proteins: Struct, Funct, Bioinf*. 2004; 57(1):128–141.
11. Glyakina AV, Garbuzynskiy SO, Lobanov MY, Galzitskaya OV. Different packing of external residues can explain differences in the thermostability of proteins from thermophilic and mesophilic organisms. *Bioinformatics*. 2007; 23(17):2231–2238. [PubMed: 17599925]
12. Narhi LO, Arakawa T, Aoki K, Wen J, Elliott S, Boone T, Cheetham J. Asn to Lys mutations at three sites which are N-glycosylated in the mammalian protein decrease the aggregation of *Escherichia coli*-derived erythropoietin. *Protein Eng*. 2001; 14(2):135–140. [PubMed: 11297671]
13. Wang L, Amphlett G, Blättler WA, Lambert JM, Zhang W. Structural characterization of the maytansinoid-monoclonal antibody immunoconjugate, huN901-DM1, by mass spectrometry. *Protein Sci*. 2005; 14(9):2436–2446. [PubMed: 16081651]
14. Acchione M, Kwon H, Jochheim CM, Atkins WM. Impact of linker and conjugation chemistry on antigen binding, Fc receptor binding and thermal stability of model antibody-drug conjugates. *MAbs*. 2012; 4(3):362–372. [PubMed: 22531451]
15. Boylan NJ, Zhou W, Proos RJ, Tolbert TJ, Wolfe JL, Laurence JS. Conjugation Site Heterogeneity Causes Variable Electrostatic Properties in Fc Conjugates. *Bioconjugate Chem*. 2013; 24(6):1008–1016.
16. Strop P, Liu S-H, Dorywalska M, Delaria K, Dushin RG, Tran T-T, Ho W-H, Farias S, Galindo Casas M, Abdiche Y, Zhou D, Chandrasekaran R, Samain C, Loo C, Rossi A, Rickert M, Krimm S, Wong T, Michael Chin S, Yu J, Dilley J, Chaparro-Riggers J, Filzen GF, O'Donnell CJ, Wang F, Myers JS, Pons J, Shelton DL, Rajpal A. Location Matters: Site of Conjugation Modulates Stability and Pharmacokinetics of Antibody Drug Conjugates. *Chem Biol (Oxford, U K)*. 2013; 20(2):161–167.
17. Adem YT, Schwarz KA, Duenas E, Patapoff TW, Galush WJ, Esue O. Auristatin Antibody Drug Conjugate Physical Instability and the Role of Drug Payload. *Bioconjugate Chem*. 2014; 25(4): 656–664.
18. Jackson D, Atkinson J, Guevara CI, Zhang C, Kery V, Moon S-J, Virata C, Yang P, Lowe C, Pinkstaff J, Cho H, Knudsen N, Manibusan A, Tian F, Sun Y, Lu Y, Sellers A, Jia X-C, Joseph I, Anand B, Morrison K, Pereira DS, Stover D. In vitro and in vivo evaluation of cysteine and site specific conjugated herceptin antibody-drug conjugates. *PLoS One*. 2014; 9(1) e83865/83861-e83865/83814, 83814 pp.
19. Junutula JR, Raab H, Clark S, Bhakta S, Leipold DD, Weir S, Chen Y, Simpson M, Tsai SP, Dennis MS, Lu Y, Meng YG, Ng C, Yang J, Lee CC, Duenas E, Gorrell J, Katta V, Kim A, McDorman K, Flagella K, Venook R, Ross S, Spencer SD, Wong WL, Lowman HB, Vandlen R, Sliwkowski MX, Scheller RH, Polakis P, Mallet W. Site-specific conjugation of a cytotoxic drug to an antibody improves the therapeutic index. *Nat Biotechnol*. 2008; 26(8):925–932. [PubMed: 18641636]
20. Krause ME, Glass AM, Jackson TA, Laurence JS. Novel Tripeptide Model of Nickel Superoxide Dismutase. *Inorg Chem*. 2010; 49(2):362–364. [PubMed: 20000358]
21. Krause ME, Glass AM, Jackson TA, Laurence JS. MAPPING the Chiral Inversion and Structural Transformation of a Metal-Tripeptide Complex Having Ni-Superoxide Dismutase Activity. *Inorg Chem*. 2011; 50(6):2479–2487. [PubMed: 21280586]
22. Krause ME, Glass AM, Jackson TA, Laurence JS. Embedding the Ni-SOD Mimetic Ni-NCC within a Polypeptide Sequence Alters the Specificity of the Reaction Pathway. *Inorg Chem*. 2013; 52(1):77–83. [PubMed: 23214928]
23. Laurence, JAS.; Vartia, AA.; Krause, ME. Metal abstraction peptide (MAP) tag and associated methods. U.S. Patent. 8,110,402. 2012 Feb 7.
24. Mills BJ, Mu Q, Krause ME, Laurence JS. *claMP* Tag: A versatile inline metal-binding platform based on the metal abstraction peptide. *Bioconjugate Chem*. 2014; 25(6):1103–1111.

25. Delaglio F, Grzesiek S, Vuister GW, Zhu G, Pfeifer J, Bax A. NMRPipe: a multidimensional spectral processing system based on UNIX pipes. *J Biomol NMR*. 1995; 6(3):277–293. [PubMed: 8520220]
26. Goddard, TD.; Kneller, DG. SPARKY. San Francisco: University of California; 2004.
27. Gill G, Richter-Rusli AA, Ghosh M, Burrows CJ, Rokita SE. Nickel-dependent oxidative cross-linking of a protein. *Chem Res Toxicol*. 1997; 10(3):302–309. [PubMed: 9084910]
28. Keil, B. Specificity of Proteolysis. Berlin; New York: Springer-Verlag; 1992.
29. Bal W, Liang R, Lukszo J, Lee S-H, Dizdaroglu M, Kasprzak KS. Ni(II) Specifically Cleaves the C-Terminal Tail of the Major Variant of Histone H2A and Forms an Oxidative Damage-Mediating Complex with the Cleaved-Off Octapeptide. *Chem Res Toxicol*. 2000; 13(7):616–624. [PubMed: 10898594]
30. Nielsen GD, Andersen O, Jensen M. Toxicokinetics of nickel in mice studied with the  $\gamma$ -emitting isotope nickel-57. *Fundam Appl Toxicol*. 1993; 21(2):236–243. [PubMed: 8405787]
31. Zweit J, Carnochan P, Goodall R, Ott R. Nickel-57-doxorubicin, a potential radiotracer for pharmacokinetic studies using PET: production and radiolabelling. *J Nucl Biol Med*. 1994; 38(4 Suppl 1):18–21. [PubMed: 7632762]
32. Krause ME, Martin TT, Laurence JS. Mapping Site-Specific Changes That Affect Stability of the N-Terminal Domain of Calmodulin. *Mol Pharmaceutics*. 2012; 9(4):734–743.
33. Skinner AL, Laurence JS. High-field solution NMR spectroscopy as a tool for assessing protein interactions with small molecule ligands. *J Pharm Sci*. 2008; 97(11):4670–4695. [PubMed: 18351634]
34. Skinner AL, Laurence JS. Probing residue-specific interactions in the stabilization of proteins using high-resolution NMR: a study of disulfide bond compensation. *J Pharm Sci*. 2010; 99(6): 2643–2654. [PubMed: 20187138]

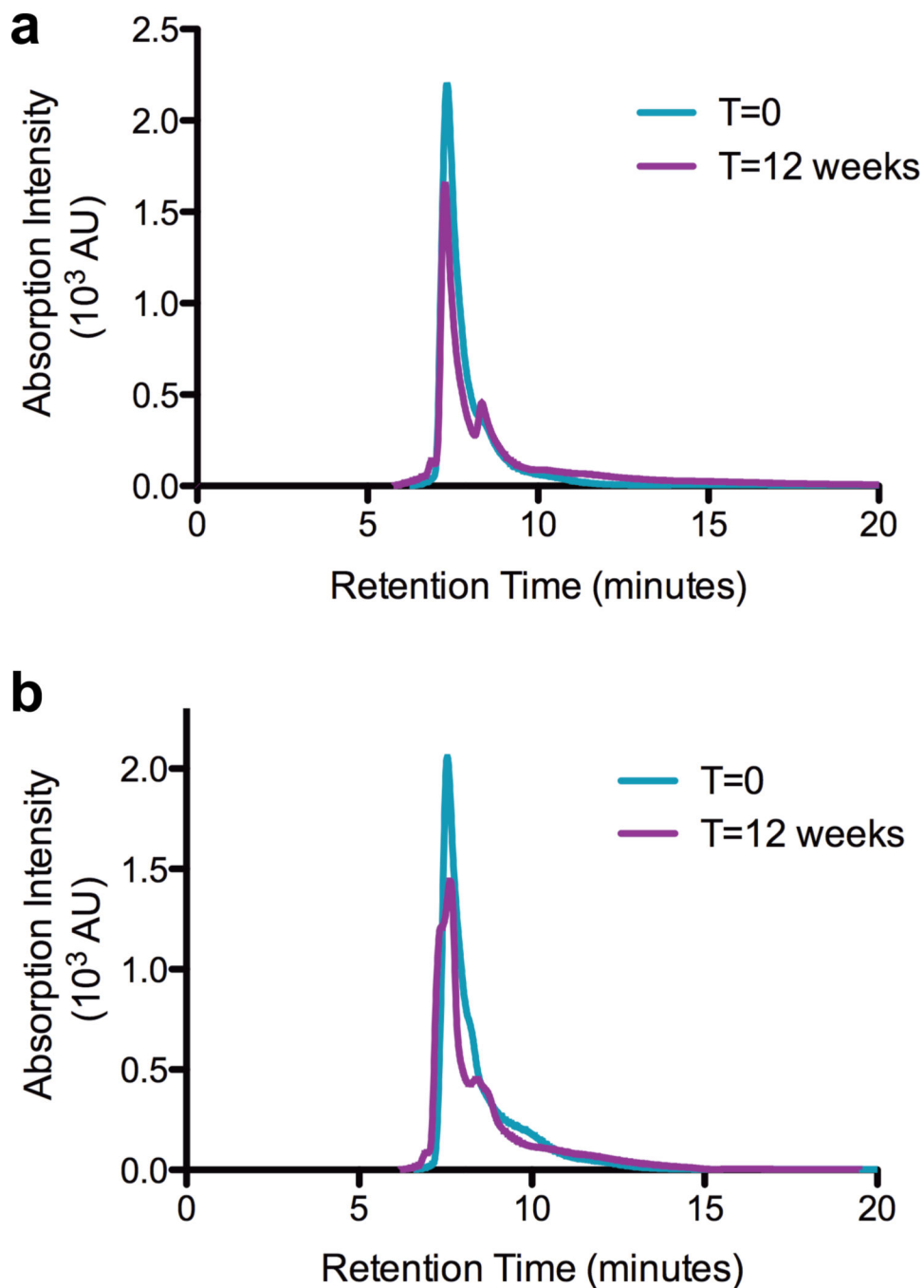


**Figure 1.** Size exclusion chromatography assessment of the monomeric content of EGF-Ni-claMP prepared in either Tris-Cl (a) or KPi (b). At the initial time point, only one species is present in both samples. After three months, mostly monomeric protein remains with the emergence of a shoulder on the backside of the peak suggests the formation of a smaller molecular weight species.

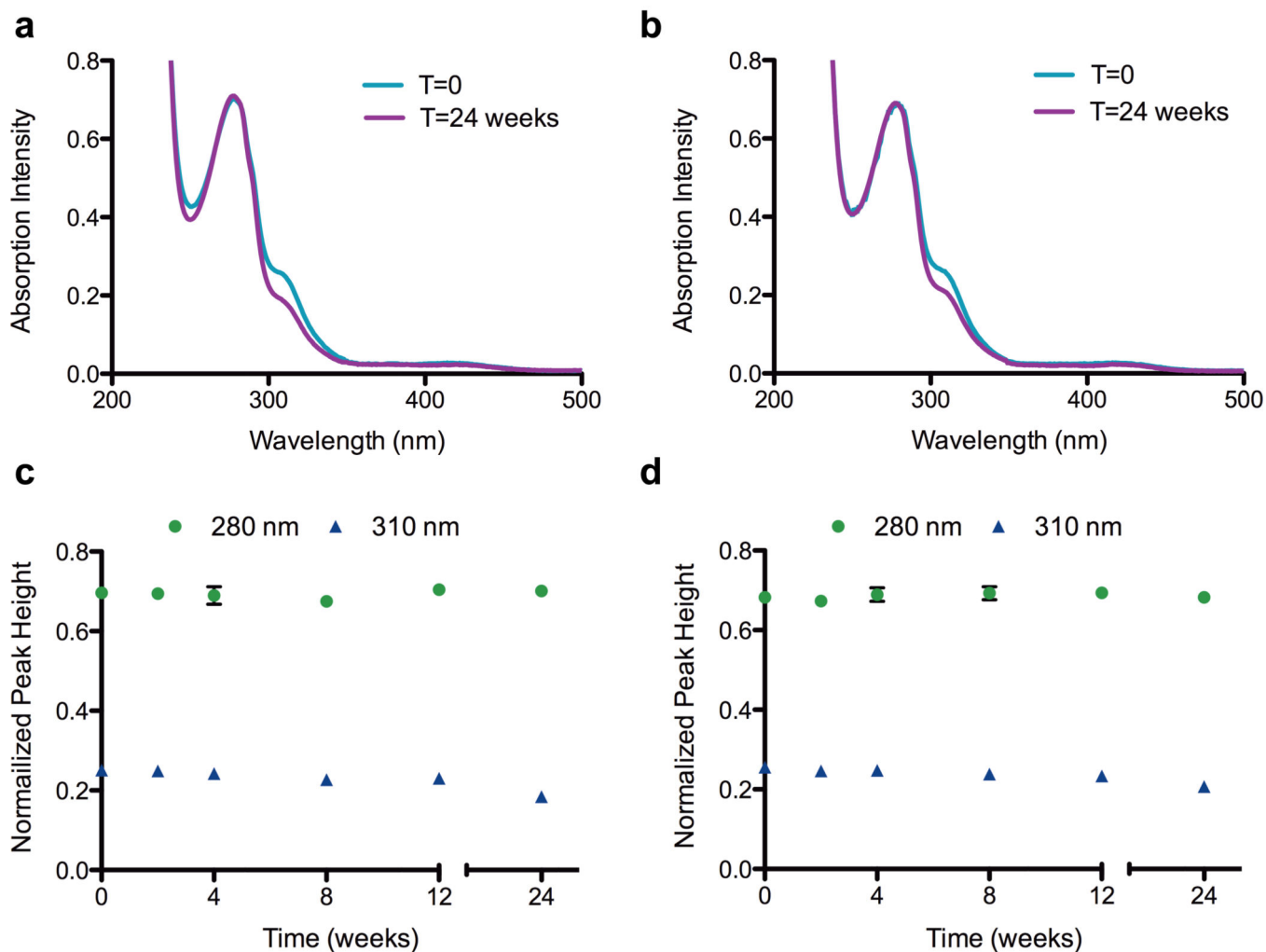


**Figure 2.**

UV-vis spectroscopy confirms Ni(II) is incorporated into the *claMP* Tag in both Tris-Cl (a) and KPi (b). Ni(II) remains incorporated in the *claMP* Tag regardless of buffer system chosen, as the intensity of the feature at 310 nm remains constant over the 12-week period with Tris-Cl (c) and KPi (d). At the 24-week time point, the intensity of the feature at 310 nm decreases, suggesting alterations occur in the Ni-*claMP* complex. The intensity of the feature at 280 nm remains constant, indicating the protein concentration remains the same over the time period investigated.

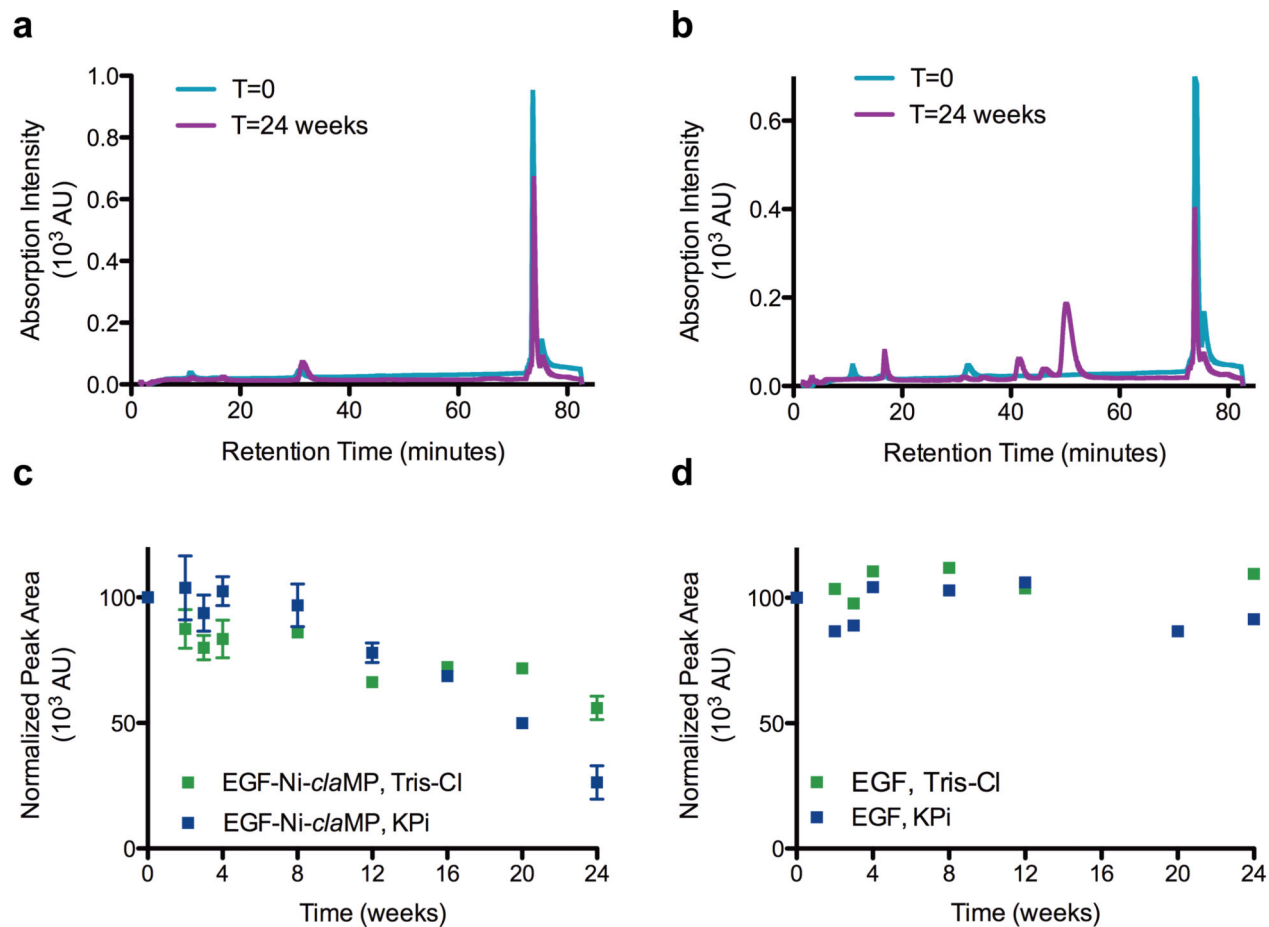


**Figure 3.**

Trend analysis by anion exchange chromatography to assess retention of intact EGF-Ni-*cla*MP. The initial chromatograms of the conjugate prepared in either Tris-Cl (a) or KPi (b) are very similar, indicating the buffer choice does not alter formation of conjugate. In the sample prepared in KPi buffer, a peak emerges at 50 minutes, indicating formation of a species with a less negative charge. c) The area of the peak at 74 minutes was plotted to reflect the amount of intact EGF-Ni-*cla*MP remaining. At 12 weeks, the area of this peak decreases by 25% and 35% for the samples prepared in Tris-Cl and KPi, respectively. At 24 weeks, the area of this peak in samples prepared in Tris-Cl and KPi decreases by approximately 40% and 70%, respectively. d) The area of the peak at 35 minutes was plotted to reflect the amount of intact EGF in solution, and it remains constant over the 24-week time period. 20% variability was observed for both EGF and EGF-Ni-*cla*MP.

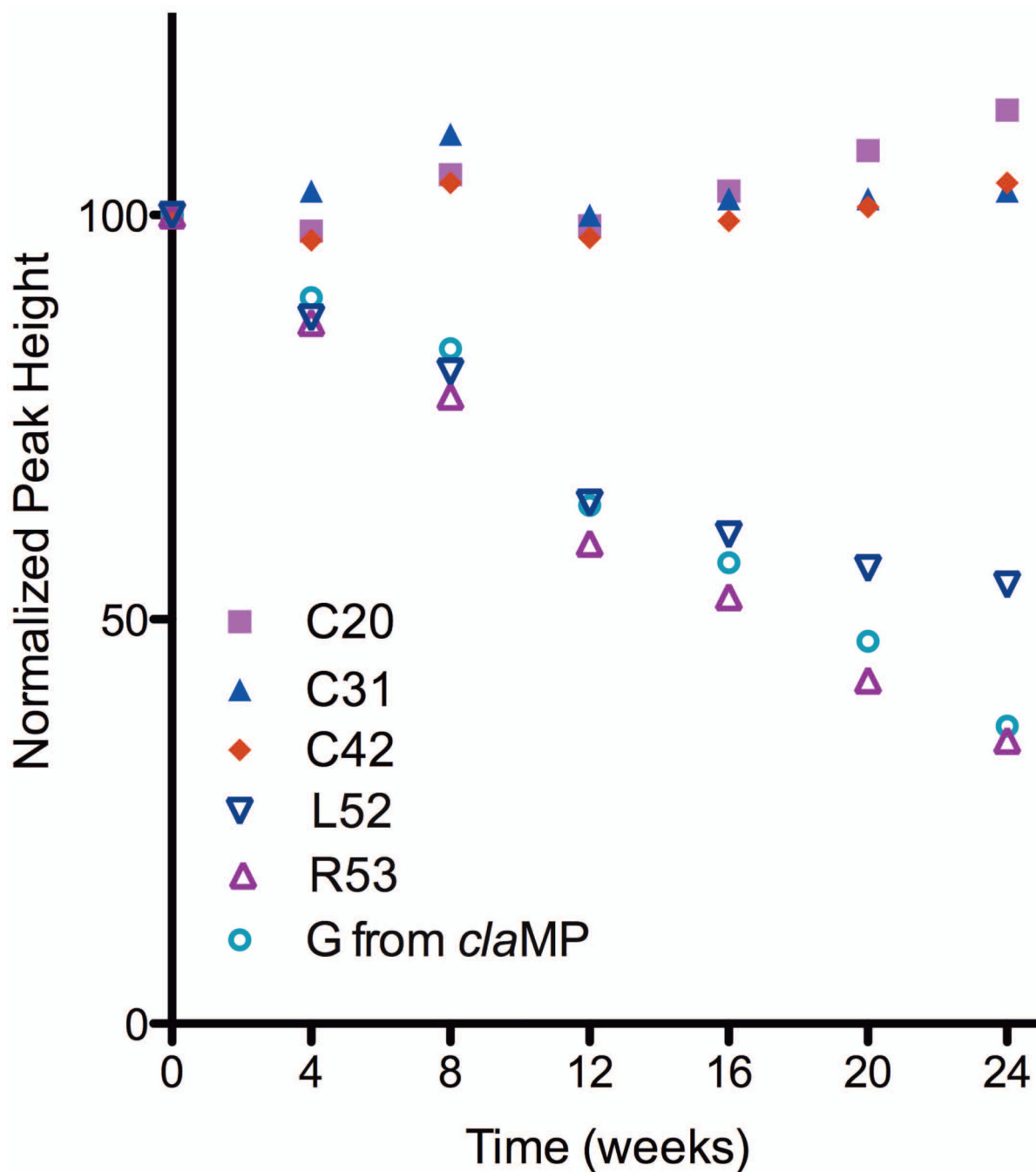


**Figure 4.** Plot of NMR peak heights. The peak height corresponding to Cys residues confirms the protein structure is maintained and no loss of protein from solution occurs. The peak heights corresponding to the Gly from the *claMP* tag and C-terminal residues from EGF (L52, R53) decrease, indicating a change in structure in this region.



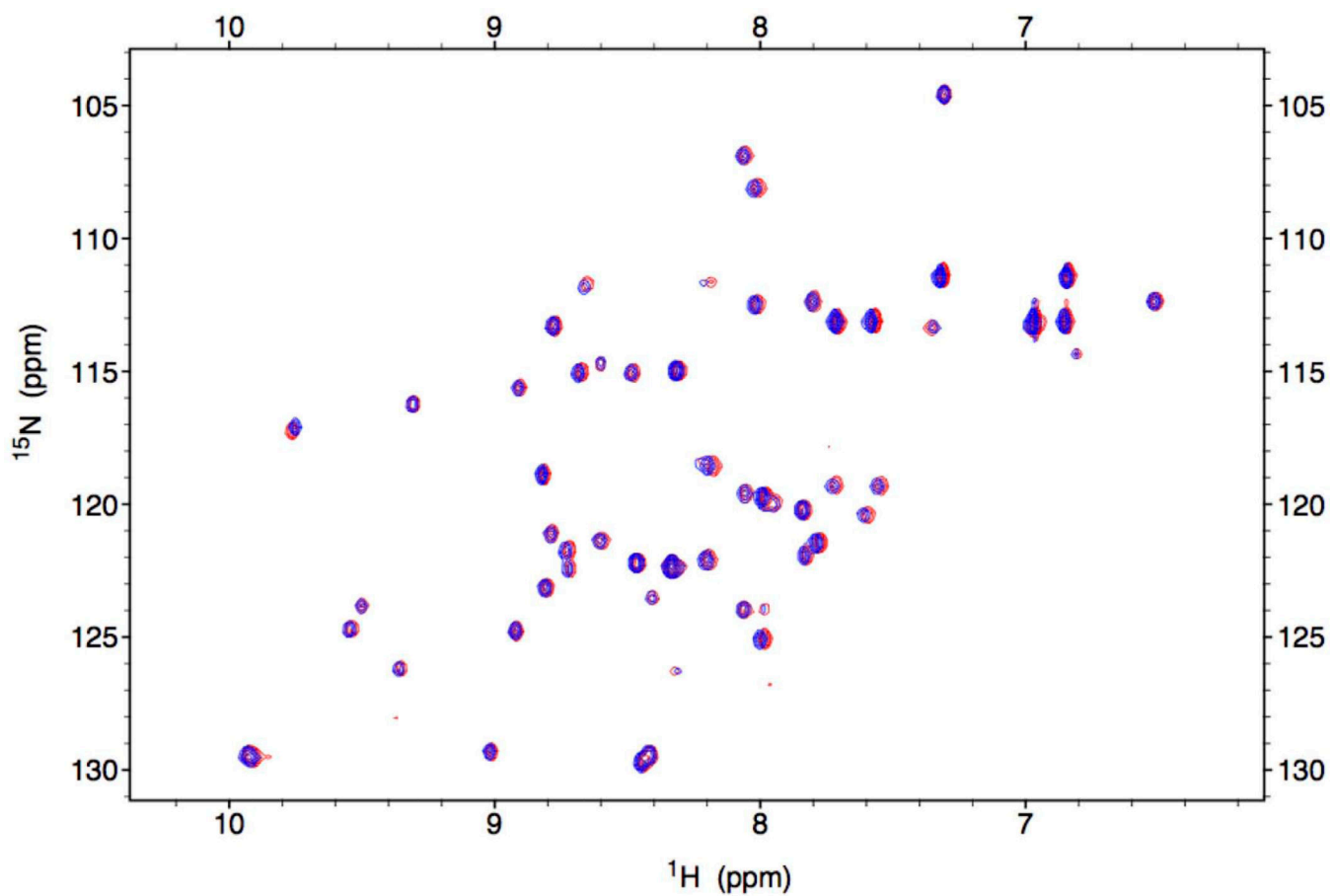


**Figure 5.**  $^1\text{H}$ - $^{15}\text{N}$  HSQC spectra confirm that buffer selection has no effect on the structure of EGF-Ni-claMP, as the peaks of the samples prepared in Tris-Cl (blue) and KPi (red) overlap completely.

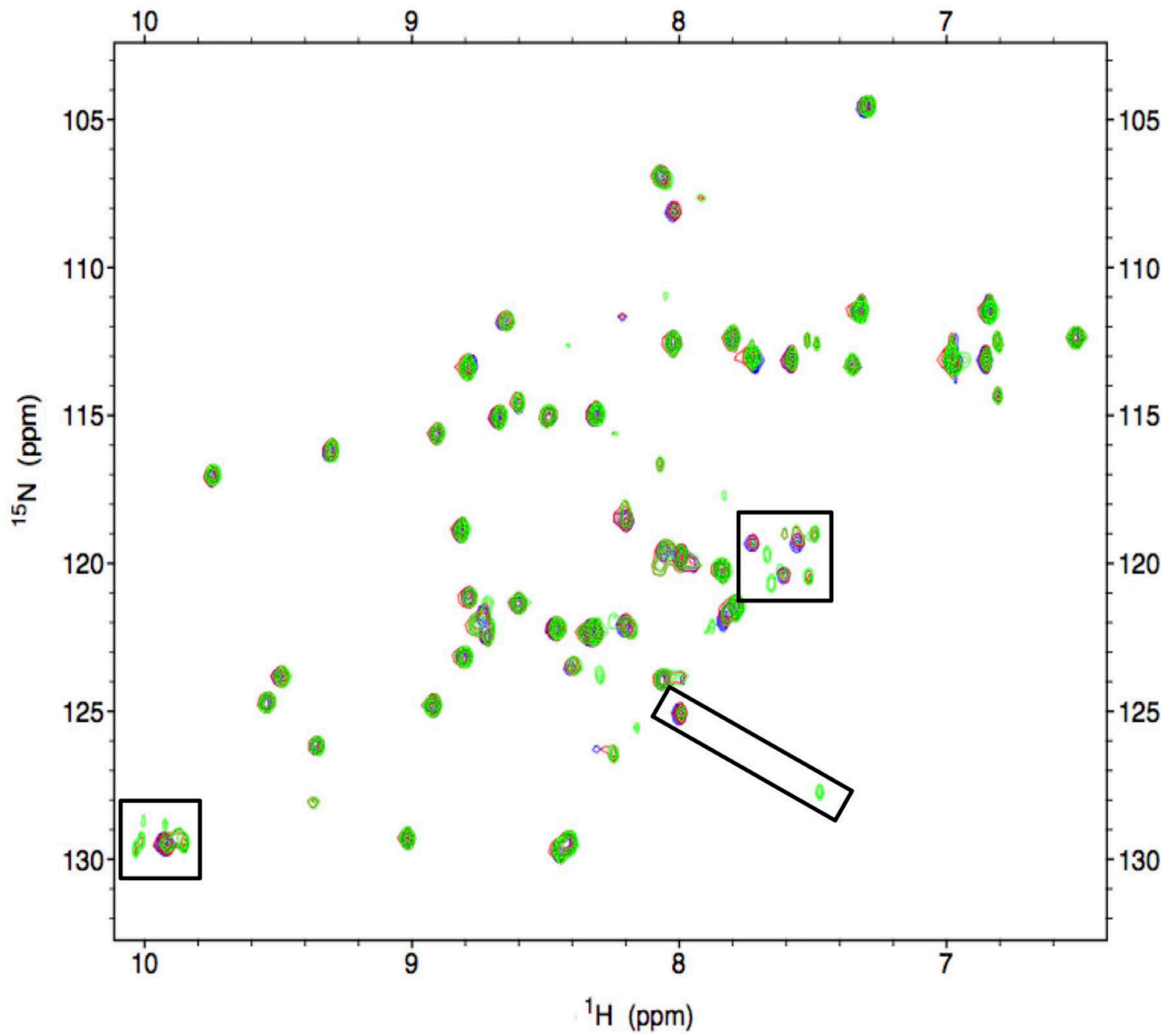


**Figure 6.**  $^1\text{H}$ - $^{15}\text{N}$  HSQC spectra of EGF-Ni-claMP at T=0 (red), T=12 weeks (blue), and T=24 weeks (green). The tertiary structure of the protein is maintained, but specific differences are observed in peaks corresponding to the C-terminal region (boxed).